

Warming automotive catalysts with pulsating flows

Benjamin, S.F. and Roberts, C.A.

Author post-print (accepted) deposited in CURVE June 2013

Original citation & hyperlink:

Benjamin, S.F. and Roberts, C.A. (2001) Warming automotive catalysts with pulsating flows. Proceedings of the Institution of Mechanical Engineers, Part D: Journal of Automobile Engineering, volume 215 (8): 891-910.

<http://dx.doi.org/10.1243/0954407011528464>

Copyright © and Moral Rights are retained by the author(s) and/ or other copyright owners. A copy can be downloaded for personal non-commercial research or study, without prior permission or charge. This item cannot be reproduced or quoted extensively from without first obtaining permission in writing from the copyright holder(s). The content must not be changed in any way or sold commercially in any format or medium without the formal permission of the copyright holders.

This document is the author's post-print version of the journal article, incorporating any revisions agreed during the peer-review process. Some differences between the published version and this version may remain and you are advised to consult the published version if you wish to cite from it.

CURVE is the Institutional Repository for Coventry University

<http://curve.coventry.ac.uk/open>

Appendix 7 Text of paper that summarises non reactive pulsating flow work

The effect of pulsating flow in warm up of non-reactive substrates, including 2D flow, is summarised by the following paper, reproduced here in full.

WARMING AUTOMOTIVE CATALYSTS WITH PULSATING FLOWS

S. F. Benjamin and C. A. Roberts

Centre for Automotive Engineering Research and Technology

School of Engineering, Coventry University, CV1 5FB, UK.

Abstract

Temperatures of an automotive catalyst substrate warmed by convection pre light-off have been measured. Direct comparison has been made of warm up by steady and pulsating flow for a 1D flow case. The 32 Hz pulsating mass flow did not feature flow reversal. Pulsations were achieved by interruption of the airflow by a rotating disc. Very small differences between steady and pulsating cases were observed because the effect of mass flow pulsations on heat transfer is minimal. Two different CFD methods were used to predict temperature. A one-dimensional porous medium model, which required input of an assumed heat transfer coefficient, was compared with a single channel model. Predictions agreed closely and there was also qualitative agreement with measurements. Similar mass flow pulsations in the range 32 to 100 Hz have been studied for a case with a larger diameter automotive catalyst supplied via a conical diffuser. The radial flow distribution is controlled by pulsation frequency and the effect of frequency on temperature at different depths in the substrate was observed experimentally. Pulsations will affect catalyst warm up in practical systems because of their effect on flow distribution, rather than on heat transfer.

Key words: automotive catalyst, pulsating flow, heat transfer, conical diffuser, exhaust systems

NOMENCLATURE

A_v	wetted surface area per unit bulk volume of substrate [m^2/m^3]
C_{pg}	specific heat of gas [$\text{J}/(\text{kg K})$]
C_w	specific heat of wall [$\text{J}/(\text{kg K})$]
d	depth in substrate [m]
D_h	channel hydraulic diameter [m]
h	heat transfer coefficient [$\text{W}/(\text{m}^2 \text{K})$]
k_g	thermal conductivity of air [$\text{W}/(\text{m K})$]
k_w	thermal conductivity of substrate wall [$\text{W}/(\text{m K})$]
m'	mass flow rate of gas per unit inlet face area [$\text{kg}/(\text{m}^2 \text{s})$]
Nu	Nusselt number (dimensionless heat flux)
T	period of pulsation [s]
T_w	wall temperature [K]
T_{wi}	wall temperature at inlet plane [K]
T_{wz}	wall temperature at location z [K]
T_g	gas temperature [K]
T_{gi}	gas temperature at inlet plane [K]
T_{go}	gas temperature at $t = 0$ at inlet plane [K]
t	time [s]

U, V, W	velocity components in x, y, z directions [m/s]
x, y, z	Cartesian co-ordinates [m]
Greek Symbols	
ϕ	parameter [$h A_v / (\rho_w C_w)$]
ε	porosity fraction
ρ_g	density of gas [kg/m ³]
ρ_m	density of substrate wall material [kg/m ³]
ρ_w	bulk density of substrate $(1-\varepsilon)\rho_m$ [kg/m ³]
ξ	Rate of rise of gas inlet temperature [K/s]

1.0 INTRODUCTION

Automotive catalyst warm up is of interest in order to achieve rapid light off. Automotive catalysts consist of a substrate coated with a washcoat to which the precious metal catalyst is applied. The substrate is either a ceramic monolith made up of a matrix of channels or a similar metallic structure. It can take up to 60 seconds for the substrate to be warmed by the gases from the engine to a temperature at which the catalyst becomes active. During this period of time unconverted exhaust escapes and so the warm up period should be minimised to reduce emissions. Studies of warm up, both measurements and CFD predictions often make the assumption that the mass flow is steady. The exhaust flow from an engine is, however, not steady. In a 4-cylinder 4-stroke engine there are two pulses per revolution and so 1000 rpm, for example, corresponds to exhaust pulsations at 33 Hz. The exhaust mass flow fluctuates approximately sinusoidally without flow reversal. The pulsation amplitude is in the region of 85 to 90% of the mean. In this study experimental measurements have been made of the warm up of an automotive catalyst substrate by steady and pulsating flow.

It can be easily demonstrated [1] for turbulent flow that heat transfer should be reduced as pulsation amplitude increases until the flow reverses, whereafter heat transfer is augmented. In most parts of an exhaust system the flow is pulsating and turbulent. There is some evidence that for exhaust systems heat transfer is augmented even without flow reversal [2]. In the automotive context the idea that pulsating flow transfers heat better than steady flow is persistent. There are parts of an exhaust system, however, where flow is laminar. The channels within an automotive catalyst experience laminar flow even under pulsating conditions.

Siegel and Perlmutter [3] studied heat transfer for pulsating laminar flow between parallel plates with constant temperature and constant flux boundary conditions. As a result of their theoretical analysis they concluded that the differences between the steady and pulsing cases were of little practical significance at high frequency, corresponding to about 35 Hz in the present study. More recent work on the effects of pulsating laminar flow in a channel on heat transfer was discussed by Kim et al. [4] who commented on the conflicting nature of the previous work that they had reviewed. Their own theoretical study, pulsating flow between parallel plates for a constant temperature input and constant temperature walls, went some way towards explaining this as they identified conditions where heat transfer was augmented and where it was decreased. The effects were, however, small. These authors reviewed only some of the literature up to that date; there had been other related studies, for example the wholly numerical studies of Sozen and Vafai [5] who considered very low pulsating flow frequency < 0.2 Hz through a packed bed. More recently, the effects of pulsations in a porous medium when there is no flow reversal have again been shown to be very small [6] for frequencies in the range 0.5 to 3 Hz. Simulation studies [7] have shown that mass flow pulsations are likely to have little influence in the case of the laminar flow in the channel of an autocatalyst substrate being warmed by a rising temperature stream, as would be the case in an engine. Most of the reports in the literature are of theoretical analyses or numerical studies. Some experimental data was reported by Hwang and Dibbs [8] but for the case where the flow oscillates and there is no net mass flow. Although overall the evidence points to there being little effect of pulsations, the real conditions in an exhaust do not correspond to the idealised cases studied. In a warming exhaust catalyst there is a net mass flow and the inlet temperature to the channels is transient.

The 1D experimental study described here was planned to provide a directly measured comparison between catalyst warm up by steady and pulsing flow. The main aim of this work was to explore experimentally the effect

of pulsating flow. A non-washcoated non-reactive ceramic substrate with cell, i.e. channel, density 62 cell/cm² (400 cpsi) was investigated. The differences between warm up achieved in the two cases have been measured and examined. The temperature rise with time of the substrate wall was recorded for the same mean flow, steady and pulsing. A hot air test rig with a flow interruption device was used to provide the pulsating flow. Predictions of the temperatures were made using the CFD package, Star-CD. Simulations were performed using two alternative models and different approaches. A single channel model provided full description of warming through every cycle by solution of a 3D conjugate heat transfer problem. These simulations were time consuming. A porous medium model (1D) ran very much more quickly but required heat transfer coefficient values as input. The steady and pulsing measurements were compared, and the results from the simulations were compared with one another and with the experimental measurements. A subsidiary aim of this work was an assessment of different modelling approaches. The results of these studies are described in this paper. Previous work [7] had suggested that pulsing flow has a minimal effect on heat transfer; this paper offers experimental evidence that confirms this.

Further experimental work has been carried out on a larger diameter automotive catalyst supplied via a conical diffuser. This type of catalyst configuration features in automotive under floor systems. Flow pulsations over the range 30 Hz to 100 Hz were investigated. Previous work on an isothermal test rig [9] had shown that the radial distribution of flow entering the substrate is affected by the pulsation frequency. Experimental results presented in this paper confirm that temperatures observed in a warming substrate are modified by pulsation frequency. The observations are consistent with different mass flows to the different parts of the catalyst.

2.0 THEORY

2.1 CFD SIMULATIONS

Two different approaches can be used to model warm up by CFD. These are the equivalent continuum porous medium approach and the single channel approach, as used by Benjamin and Roberts in [7] and [10] respectively. Both of these alternative CFD models were used in these studies. The first model was a quarter of a single square channel. The second was essentially a porous medium model, based on a technique described by Clarkson [11]. The simulations were confined to laminar flow conditions.

The meshes used are shown in Figs. 1 and 2. The quarter square channel (Fig. 1) had a half side width of 0.554 mm and a wall half thickness of 0.081 mm, i.e. the substrate had channels of square cross section with hydraulic diameter 1.108 mm and wall thickness of 0.162 mm. There were 9 cells comprising the quarter channel and 7 cells around the quarter wall. In the axial direction (z co-ordinate) there were 4 cells of 1 mm length at inlet, followed by 60 cells over the 84 mm length of the walled channel. This model thus featured 1024 cells in total. The porous medium model (Fig. 2) was a cell block with dimensions 5 mm x 5 mm x 170 mm representing the fluid, plus cell block with dimensions 5 mm x 5 mm x 150 mm representing the solid. The fluid block had 4 cells over 10 mm length at inlet with air properties, plus 60 cells over 150 mm with air properties and porous medium flow resistance properties, and finally 4 cells over 10 mm length at exit with air properties. The solid block had 60 cells. The whole model with two cell blocks totalled only 128 cells. The parameters for the two models are listed in Table 1.

In the previous work [7] the single channel was represented by a sector of a circular channel, whereas here the channel is a quarter square channel set with channel axis and flow in the +z direction. The single channel simulations represent a case of uniform flow across the substrate face under adiabatic conditions. Thus a single channel is representative of the whole substrate. The flow within the channel is fully 3D and is represented as follows. The conduction equation for the substrate wall is,

$$k_{wx} \frac{\partial^2 T_w}{\partial x^2} + k_{wy} \frac{\partial^2 T_w}{\partial y^2} + k_{wz} \frac{\partial^2 T_w}{\partial z^2} = \rho_w C_w \frac{\partial T_w}{\partial t} \quad (1)$$

The energy equation describing the gas is

$$k_{gx} \frac{\partial^2 T_g}{\partial x^2} + k_{gy} \frac{\partial^2 T_g}{\partial y^2} + k_{gz} \frac{\partial^2 T_g}{\partial z^2} = \rho_g C_{pg} \left[\frac{\partial T_g}{\partial t} + W \frac{\partial T_g}{\partial z} \right] \quad (2)$$

At the interface between the gas and the wall, the specified boundary condition is continuity of heat flux; conjugate heat transfer is assumed at the gas/wall interface. The outer solid surfaces of the model (substrate wall mid-line) were set as adiabatic boundaries and the mid-channel fluid boundaries were defined as symmetry planes.

For the porous medium model as used in this study, the treatment was wholly 1D; the problem is expressed in terms of simultaneous gas and solid equations. The co-ordinate system is set up so that the substrate axis and flow are in +z direction. The conduction equation for the substrate wall in an isotropic continuum is,

$$(1-\varepsilon) k_{wz} \frac{\partial^2 T_w}{\partial z^2} + h A_v (T_g - T_w) = \rho_w C_w \frac{\partial T_w}{\partial t} \quad (3)$$

The energy equation describing the gas is

$$\varepsilon k_{gz} \frac{\partial^2 T_g}{\partial z^2} = \rho_g \varepsilon C_{pg} \left[\frac{\partial T_g}{\partial t} + W \frac{\partial T_g}{\partial z} \right] + h A_v (T_g - T_w) \quad (4)$$

In the porous medium model all the boundaries, both solid and fluid, were set as adiabatic; the heat transfer was calculated within user subroutines using the heat transfer coefficient. The wetted area per unit volume of the porous medium, A_v was $2750 \text{ m}^2/\text{m}^3$. The heat transfer coefficient, h was found from Nusselt number 3.608, which is the value for Nu (H1) for fully developed flow in a square channel [12]. Within the simulation, the mean of the gas and wall temperature was determined and from this a local value for k_g (W/(m K)) was found. The local value for the heat transfer coefficient was then found from $h = k_g \text{Nu} / D_h$ where D_h is 0.001108 m for the square channel. The heat transfer coefficient values were then elevated by 1.9, 1.4, 1.2, 1.15 and 1.1 respectively in the first five 2.5 mm length cells. This made an allowance for higher heat transfer coefficient values in the entrance region.

In the CFD models the inlet boundary conditions for velocity components and temperature are:

$$\begin{aligned} U &= 0 \\ V &= 0 \\ W &= W_{mean} + W_{amp} \sin(2 \pi t/T) \\ T_{gi} &= T_{gi}(t) \end{aligned}$$

The mean velocity, W_{mean} was 2.4 m/s and amplitude, W_{amp} was 2.04 m/s (85 % of mean) as measured at 293 K. The flow through the catalyst channel was laminar with Reynolds number 230 corresponding to the mean flow. The inlet velocity varied directly with inlet temperature so that the net mass flow remained unchanged.

In both models the initial temperatures were $T_g = 299 \text{ K}$ and $T_w = 293 \text{ K}$. The CFD simulations were run as transient cases using the PISO algorithm [13]. In the pulsating simulations the time step was 0.00078125 s. Thus 64000 time steps spanned 50 s. The cell length in the quarter square channel model was 1.4 mm and 2.5 mm in the porous medium model so that the Courant No. was $\ll 50$ throughout the pulsating simulations. The upwind differencing scheme was used for the quarter square channel model but this is justifiable for laminar channel flows. In the porous medium model the upwind differencing scheme was also used but in this case central differencing was used for temperature.

The steady mass flow was input initially as a steady velocity of 2.34 m/s at 293K. The velocity thereafter varied directly with inlet temperature so that the mass flow remained unchanged. In the first steady simulations using the quarter square channel model the time step was 0.003125 s. so that there were 16000 time steps spanning 50 s. Identical results were, however, obtained with a time step of 0.0125 s. so that 4000 time steps spanned 50 s. This longer time step speeded up the simulations for the quarter square channel model. The Courant No. was higher in the steady simulations but was < 50 throughout. The models were run on an SGI Indy Workstation with 256 MB RAM and R5000 processor. The quarter square channel model was slow to run, taking several days even for the steady cases, whereas the porous medium model ran in only a couple of hours.

2.2 PLOTTING THE EXPERIMENTAL RESULTS

If there is only a small difference between the warming achieved by steady and pulsating flow, then it will be necessary to plot observed temperatures in a way that exposes that difference.

It can be shown [10] assuming negligible heat conduction that at the inlet plane where $z = 0$

$$T_{wi} = \frac{\xi}{\phi} (e^{-\phi t} - 1) + \xi t + T_{go} \quad (5)$$

$$= \frac{\xi}{\phi} (e^{-\phi t} - 1) + T_{gi} \quad (6)$$

where the parameter $\phi = (hA_v)/(\rho_w C_w)$. It follows that

$$T_{gi} - T_{wi} = \frac{\xi}{\phi} (1 - e^{-\phi t}) \quad (7)$$

If ϕt is small, ≤ 0.05 , then $T_{gi} - T_{wi} \approx \xi t$

but if ϕt is large, ≥ 3 , then

$$T_{gi} - T_{wi} \approx \frac{\xi}{\phi} \quad \text{and} \quad \frac{dT_w}{dt} \approx \xi \quad (8)$$

For typical values of ξ found in practical systems the heat flux may be assumed to be approximately constant along the channel [10]. At large times and away from the inlet plane where $z > 0$

$$T_{wz} = T_{wi} + z \frac{dT_w}{dz} \quad (9)$$

$$\approx T_{wi} + z \frac{dT_g}{dz} \quad (10)$$

$$T_{gi} - T_{wz} \approx T_{gi} - T_{wi} - z \frac{dT_g}{dz} \quad (11)$$

Furthermore it was demonstrated in [10] that at large times

$$\frac{dT_g}{dz} = - \frac{\xi \rho_w C_w}{m' C_{pg}} \quad (12)$$

It follows that

$$T_{gi} - T_{wz} = \frac{\xi}{\phi} + \frac{\xi \rho_w C_w z}{m' C_{pg}} \quad (13)$$

$$= \xi \rho_w C_w \left[\frac{1}{h A_v} + \frac{z}{m' C_{pg}} \right] \quad (14)$$

The pulsations could influence the difference between the inlet gas temperature and the wall temperature through the m' term or through the value for coefficient h .

The inlet gas temperatures in the steady and pulsing experiments were very similar but were not identical. Therefore the experimental data was plotted as $T_{gi} - T_{wz}$ against time in an attempt to make some allowance for small differences in T_{gi} from case to case. Plotting $(T_{gi} - T_{wz})/\xi$ was also investigated as the rate of rise of inlet temperature with time also differed slightly from case to case.

For the cases using the conical diffuser, the results were plotted as a temperature ratio

$$\frac{T_{gi} - T_{wz} (d = 0.045)}{T_{gi} - T_{wz} (d = 0.015)} \quad (15)$$

where 0.015 and 0.045 m are depths in a substrate cylinder of 0.118 m diameter. This enabled the relative warming of different parts of the substrate to be clearly revealed.

3.0 EXPERIMENTAL METHOD

3.1 THE 1D STUDIES

The hot air flow test rig has been described in a previous paper [14]. This has been modified by the inclusion of a rotating disc system that interrupts the flow, see Fig. 3. A dc motor drives the disc. The cast iron disc is about 6 mm thick and supports four plates with holes in. In each quarter of the plate's rotation one pulse is produced by the hole being fully open for 15.1 % of the period, fully closed for 15.1 % of the period and partially open/closed for 34.9 % of the period between the fully open and fully closed phases. When the disc rotates at 8 cycles per sec 32 Hz pulses are generated that are approximately sinusoidal. An example of the waveform of the pulsating flow is shown in Fig. 4. The rotation frequency of the disc is monitored and the open and closed phases of the plate are logged.

The inlet air temperature ramps measured in the experiments are shown in Fig. 5. These were obtained from 0.5 mm K-type thermocouples located just upstream of the substrate. It was assumed that the passage of the rotating disc simply pulsed the mass flow but did not generate temperature pulsations. Experiments 1 & 2 were both pulsing and average temperature values are presented. Experiment 3 was a steady flow experiment. Experiments 4 & 5 were steady flow experiments for which averages are presented. The inlet temperature ramps are seen from Fig. 5 to be similar but not identical. This was because in practice the test rig provided slightly different ramp shapes for steady and pulsing flow cases. Adjustment was by trial and error by preheating a can containing nine electrical elements for various times prior to the airflow and by using different combinations of elements. The flow velocity in the experiments was measured with a hot wire anemometer. A viscous flow meter in the air line upstream of the test rig was used to monitor the mass flow rate but a hot wire was inserted into the duct about 20 mm upstream of the catalyst substrate for velocity measurements. Measurements indicated velocities of 2.4 ± 0.1 m/s mean for pulsing flow but 2.34 ± 0.02 m/s for steady flow. The velocity profiles across the duct differed slightly between steady and pulsing cases but close matching at 15 mm depth was achieved.

Substrate wall temperatures were measured by 0.5 mm diameter K type thermocouples. Fig. 6 shows the results of the experimental measurements. The ceramic substrate sample was 50 mm diameter and 150 mm length and the thermocouples were inserted to 15 mm depth through 0.7 mm holes and were taped so that their tips were forced into contact with a channel wall. It can be seen in Fig. 6 that the warm up appears to be initially faster in the pulsating case where the inlet temperature ramp is slightly steeper, Fig. 5.

3.2 STUDIES USING CONICAL DIFFUSER

Measurements were made on an isothermal flow rig [9] of the velocity profile at exit from a substrate supplied with air via a conical diffuser. Controlled pulsations were achieved by interruption of the flow with a rotating disc. The experiments showed much less maldistribution of the velocity profile for pulsating flow than for the steady flow case. These studies showed very significant flattening of the velocity profile at 100 Hz. This effect was observed unequivocally but CFD simulations do not predict correctly this effect on the flow field in the diffuser and hence at entry to the substrate. This is the subject of ongoing work. As the inability to correctly predict velocity is known, then there is little value in attempting to predict temperature at this stage. Hence the temperatures achieved by pulsating flows reported here are experimental only.

The conditions for the tests are summarised in Table 2. The inlet temperature ramps were recorded for the six experiments in the 48 mm diameter supply duct. A conical diffuser expanded the duct size from 48 to 118 mm diameter over a length of 60 mm so that the cone angle was approximately sixty degrees. The non-washcoated ceramic substrate was 118 mm diameter and 150 mm length. Thermocouples (0.5 mm K type) probed the substrate such that in each experiment the temperature was measured at either 15 mm or 45 mm depth in the substrate. The thermocouples measured the temperatures at specified distances into the catalyst, i.e. at $z =$

13,18,30, 43 and 78 mm. The thermocouples were placed in the same diametral plane for which velocity measurements were obtained, see later.

4.0 RESULTS

4.1 THE 1D RESULTS

Fig. 7 shows measured wall temperatures compared with CFD predictions for steady case 3. Fig. 8 shows measured wall temperatures compared with CFD predictions for steady experiments 4 & 5. Fig. 9 shows measured wall temperatures compared with CFD predictions for the pulsing experiments 1 & 2. Figs. 7 – 9 show that very good agreement was achieved between the two independent CFD models. As has been previously observed [14] the monolith is warmed faster than predicted initially by the steady flow, but its temperature lags behind the predicted values at later times. The pulsing case, Fig. 9, shows a similar trend. From these plots no highly significant difference is apparent in the behaviour of the steady and pulsing cases.

Fig. 10 shows a comparison of measured data for steady case 3 and the pulsing case but plotted as $[T_{gi} - T_w]$ as a function of time. Fig. 11 is the corresponding plot where experiments 4 & 5 are compared with the pulsing case. These plots exhibit similar features and both show that the measured value for $[T_{gi} - T_w]$ is larger for the pulsating case than for the steady cases in the first 5 to 10 seconds when the inlet temperature is rising rapidly with time. These differences and those at later times may, however, be attributable to differences in the value for ξ , the inlet temperature ramp, as indicated in equation (15).

Fig. 12 shows a comparison between the steady and pulsing CFD predictions from the porous medium model plotted as $[T_{gi} - T_w]$. Fig. 13 shows a comparison between the steady and pulsing CFD predictions from the quarter square single channel model also plotted in this way. The good agreement between the two CFD models is again demonstrated as the figures are almost identical. Figs. 12 and 13, the results from the simulations, indicate good qualitative agreement with Figs. 10 and 11, the results from the experimental measurements. Figs. 12 and 13 indicate less effective warming in the case of the pulsating flow in the first 10 seconds, but only small differences between the steady and pulsing flows at later times. Fig. 14 shows some results from numerical simulations done using the inlet temperature ramp corresponding to the pulsating case, but run additionally for steady flows of 2.34 and 2.4 m/s. This plot confirms that the effect of the small difference in flow rate is negligible. It does, however, imply that the small differences between the steady and pulsing observations and also between the steady and pulsing simulations may be due to inlet temperature ramp differences, see Fig. 5, rather than to the pulsations themselves intrinsically. Fig. 15 shows a plot of experimental data for $[T_{gi} - T_w]/\xi$ for the two steady and the pulsing cases. Eliminating the effect of the inlet gas temperature ramp in this way confirms that the steady and pulsing cases are not significantly different.

4.2 RESULTS USING CONICAL DIFFUSER

Figure 16 shows the inlet temperature ramps for the experiments listed in Table 2. Figure 17 shows normalised velocity profiles at the substrate exit, measured in the same plane as the substrate temperatures. The mean velocity w_{mean} used for normalisation was obtained from integration of the velocity profiles in each case. Figure 18 shows plots of the value of ratio (15) for each frequency investigated. The ratios at the three frequencies investigated are clustered around particular values at high times. More uniform values for solid temperatures in the substrate, i.e. ratios nearer to unity, are observed at higher frequencies. This is consistent with the flatter velocity profiles [9] that have been observed at higher frequencies, see Figure 17. This occurs because the mass flow per channel is more nearly uniform across the substrate at higher frequency. Warm up is therefore likely to be more uniform in a substrate supplied via a diffuser when the flow is pulsating at higher frequency.

5.0 CONCLUSIONS

The two different 1D CFD simulations using a quarter square single channel model and a porous medium model gave very good agreement one with the other. The experimental measurements and the CFD predictions showed only small differences between the steady and pulsing cases. In the cases investigated, the pulsating mass flow had an amplitude of about 85 % of the mean so that there was no flow reversal. The pulsating flow appeared to be less good at warming the substrate than the steady flow in the first 5 to 10 seconds when the inlet temperature was rising rapidly. Although the observations suggested that steady flow warms the substrate more effectively than pulsating flow in the early stages of warm up, the effect was found to be attributable to small differences in gas inlet temperature ramp. The gas inlet temperature ramp is a powerful parameter in controlling the warm up of the substrate. The experimental data presented in this paper confirm that the effect on heat transfer during

warm up caused by mass flow pulsations is small and would not be significant in the practical situation of catalyst warm up. When making CFD predictions for real systems, use of steady flow rather than pulsing flow would introduce negligible error and would have the advantage of providing significant reductions in computational effort.

The situation is different in the case with the conical diffuser. A practical catalyst configuration of this type experiences a different velocity distribution at the catalyst inlet face in the pulsating flow case from the steady flow case. This more complex situation was studied at 30, 60 and 100 Hz. Measurements showed that the temperatures noted in different parts of the catalyst were dependent upon frequency. The observations were consistent with the flow profile changes that are known to occur with pulsation frequency.

This paper has presented mainly experimental observations. Attempts to predict the correct flow and temperature field in pulsating systems with conical diffusers are the subject of ongoing work.

Acknowledgements

The authors acknowledge Arvin Exhaust Ltd., Ford Motor Company, Jaguar Cars Ltd., and Johnson Matthey plc; the project is supported under the SERC-DTI Link Programme on Applied Catalysis which is currently funding the research project.

Table 1

Parameters for CFD simulations

	Quarter channel		Porous medium
Wall specific heat J/(kgK)	1100	Solid specific heat J/(kg K)	1100
Wall Density kg/m ³	1750	Bulk density kg/m ³	420
Wall conductivity W/(m K)	1.4	Axial conductivity W/(mK)	0.34
Channel Area (mm ²)	1.108 ²	Porosity %	76.0
Cell density (cells/ cm ²)	62		

Table 2

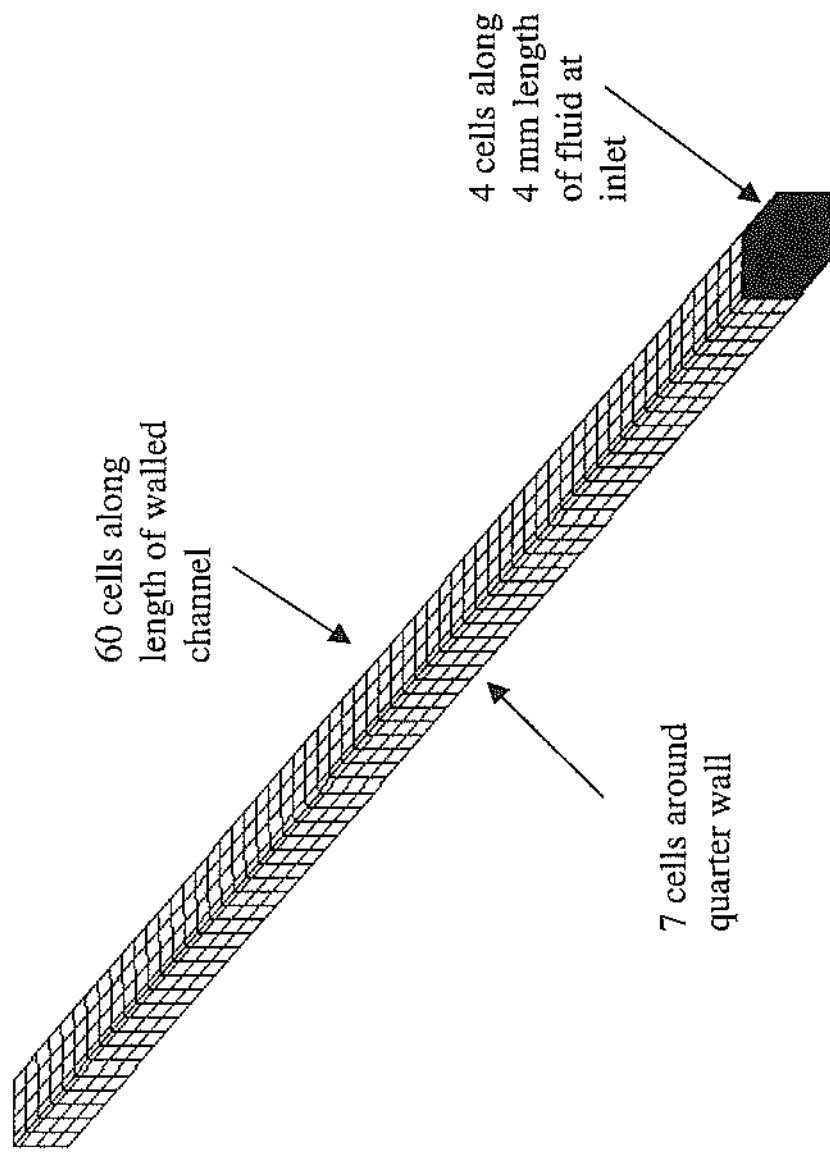
Summary of tests with conical diffuser upstream of 118 mm diameter substrate

Frequency Hz	Thermocouple Depth mm	Estimated overall mean exit velocity m/s	Re No. in inlet pipe
30	45	2.08	39,800
29	15	2.03	38,800
100	15	2.71	51,800
98/100	45	2.73	52,200
59	45	2.19	41,900
59	15	2.20	42,000

References

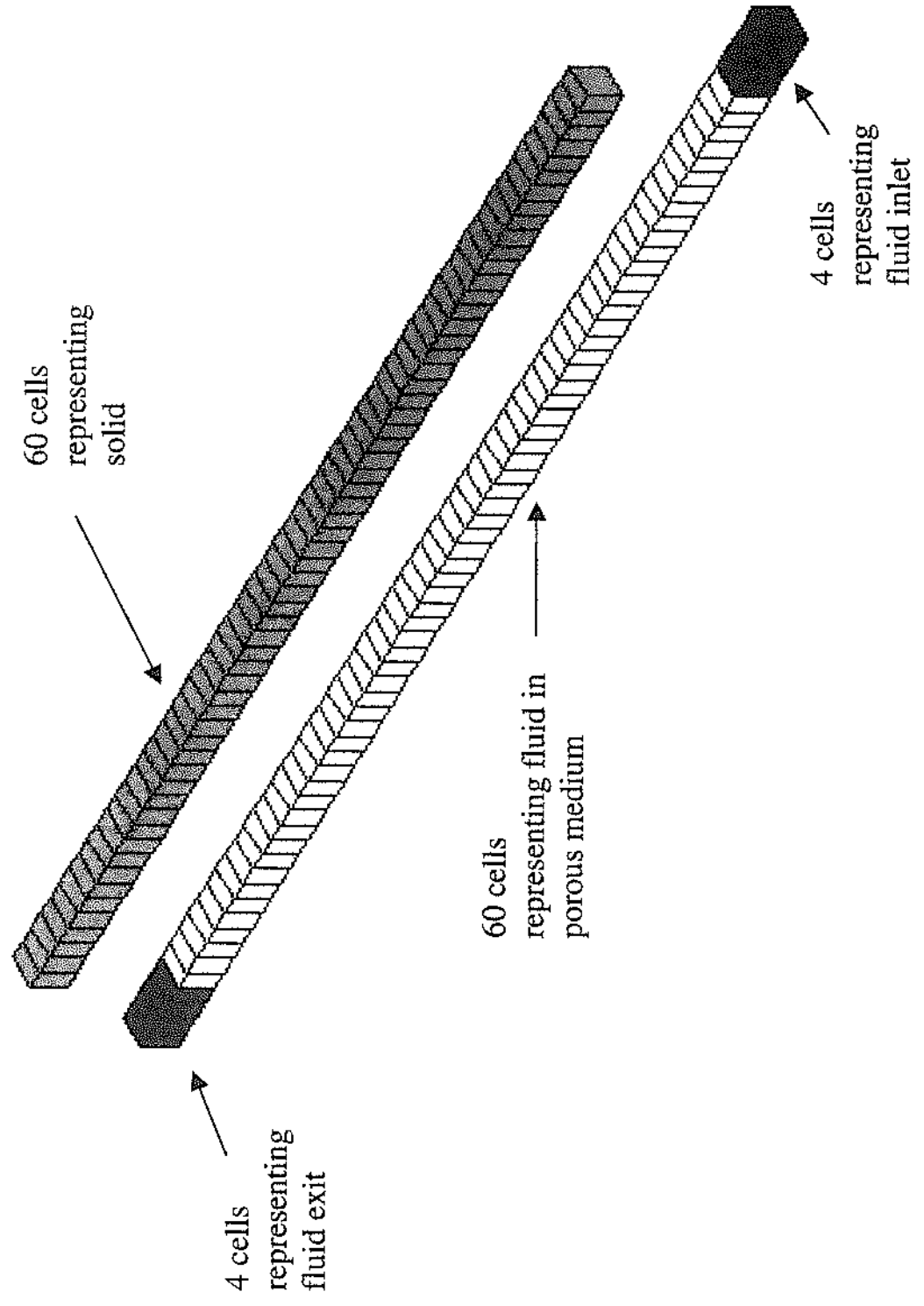
- [1] V. I. Hanby. Convective heat transfer in a gas fired pulsating combustor. *Transactions ASME Journal of Engineering for Power* January (1969) 48 – 52
- [2] K. G. Condie. K. A. Shipnaugh. D. M. McEligot. Convective heat transfer for pulsating flow in an exhaust system component. *Vehicle Thermal Management Systems Conference* (1995). VTMS Proceedings, Paper C496/062/95, 625 –636
- [3] R. Siegel. M. Perlmutter. Heat transfer for pulsating laminar flow. *Trans ASME Journal of Heat Transfer* (1962) 111 - 123

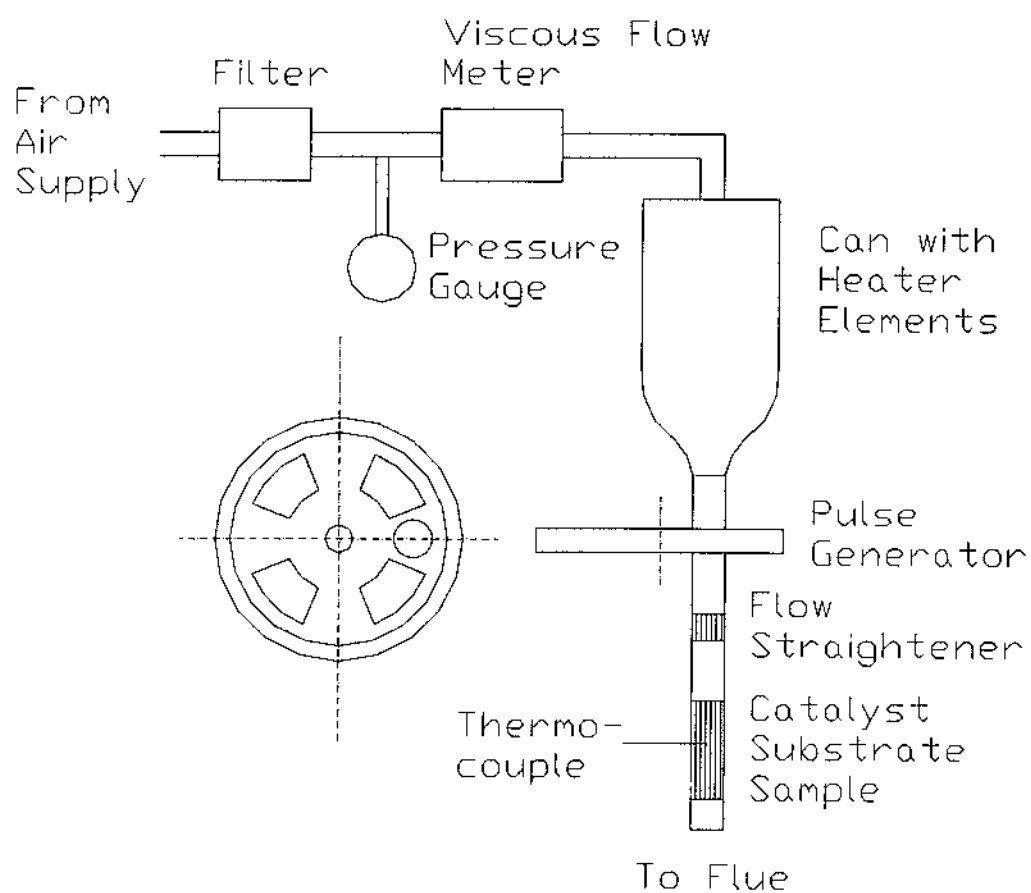
- [4] **S. Y. Kim, B. H. Kang, J. M. Hyun.** Heat transfer in the thermally developing region of a pulsating channel flow. *International Journal of Heat and Mass Transfer* 36 (1993) 4257 – 4266
- [5] **M. Sozen, K. Vafai.** Analysis of oscillating compressible flow through a packed bed. *International Journal of Heat and Fluid Flow* 12(2) (1991) 130 - 136
- [6] **J. W. Paek, B. H. Kang, J. M. Hyun.** Transient cool down of a porous medium in pulsating flow. *International Journal of Heat and Mass Transfer* 42 (1999) 3523 – 3527
- [7] **S. F. Benjamin, C. A. Roberts.** Warm up by pulsating flow of an automotive catalyst substrate: A single channel modelling approach. *International Journal of Heat and Fluid Flow* 21 (2000) 717 – 726
- [8] **M. F. Hwang, A. Dybbs.** Heat transfer in a tube with oscillatory flow. *ASME Paper* 83-WA/HT-90 (1983) 1 - 12
- [9] **S. F. Benjamin, C. A. Roberts, J. Wollin.** A study of pulsating flow in automotive catalyst systems. *Submitted to Experiments in Fluids.* (2000)
- [10] **S. F. Benjamin, C. A. Roberts.** Modelling warm up of an automotive catalyst substrate using the equivalent continuum approach. *International Journal of Vehicle Design* 22 (1999) 253 - 273
- [11] **R. J. Clarkson.** The implementation of a reacting catalyst model within Star-CD. *Computational Dynamics Ltd. Report* CD96/999/R4 (1996)
- [12] **R. K. Shah, A. L. London.** Laminar flow forced convection in ducts (*Advances in Heat Transfer – Supplement 1*). *Academic Press Inc.* (1978)
- [13] **R. I. Issa.** Solution of the implicitly discretised fluid flow equations by operator splitting. *Journal of Computational Physics* 62 (1986) 40 – 65
- [14] **S. F. Benjamin, C. A. Roberts.** Warm up of automotive catalyst substrates: Comparison of measurements with predictions. *International Communications in Heat and Mass Transfer* 25 (1998) 19 – 32



Appendix 7 Fig. 1 Mesh for quarter square single channel model

Appendix 7 Fig. 2 Mesh for porous medium model





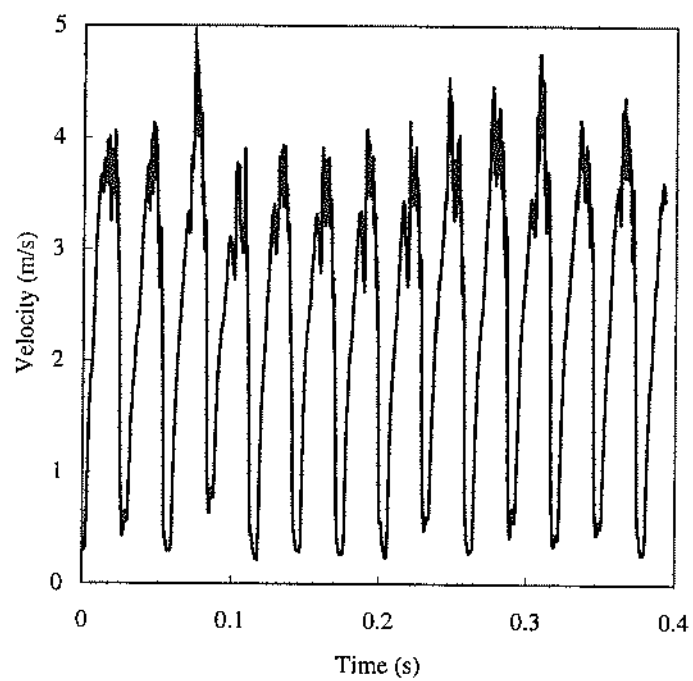
Appendix 7 Fig. 3

Schematic diagram of test rig including rotating disc system

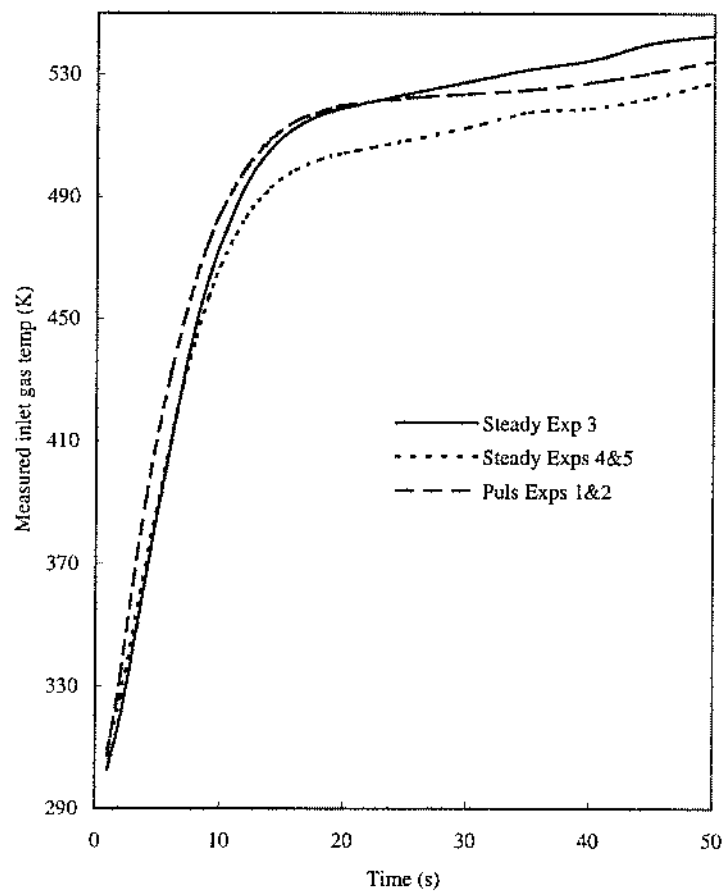
Appendix 7

Fig. 4

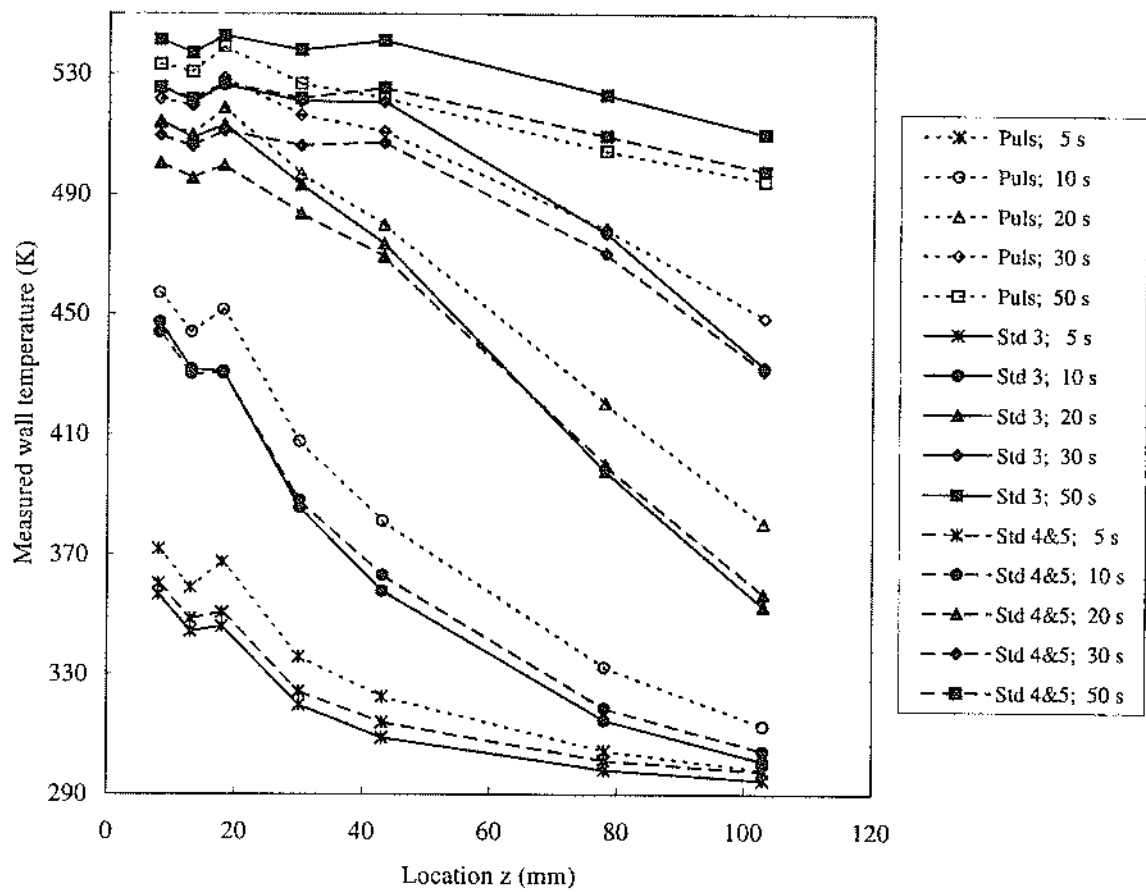
**Example of velocity pulsations
achieved by interruption of flow by rotating disc system**



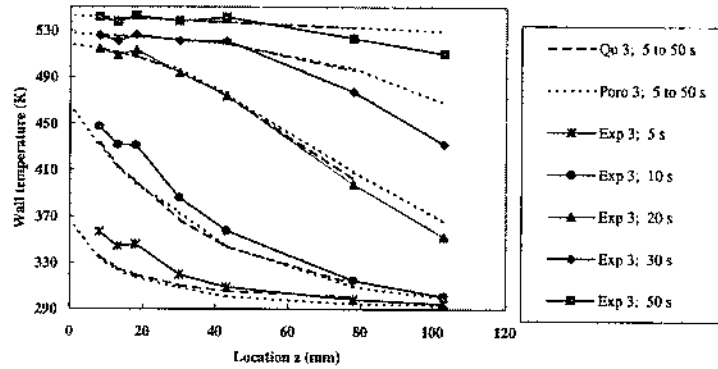
Inlet air temperature ramps



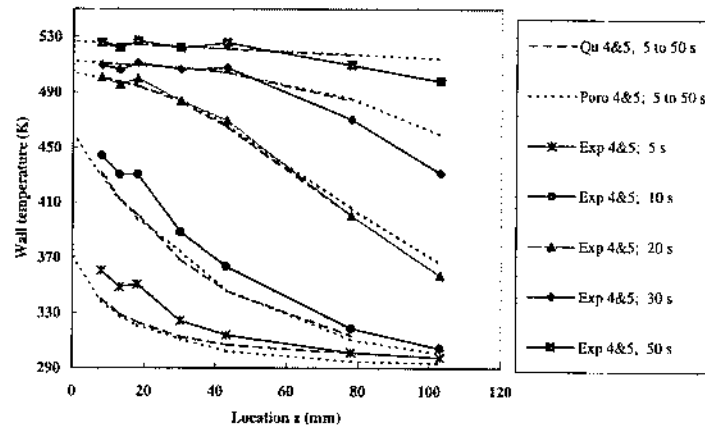
Appendix 7 Fig. 6
Measured wall temperatures at times between 5 and 50 secs.



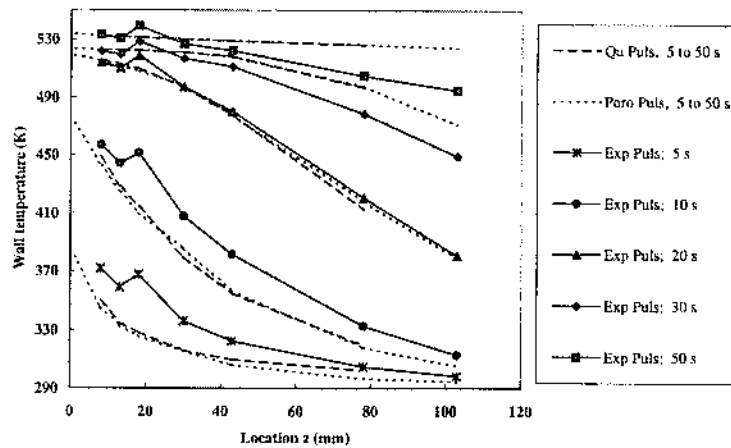
Appendix 7 Fig. 7
 Measured wall temps. from Steady Expt. 3 compared with predictions from
 two different CFD models
 [Qu, single channel model] Poro, porous medium model]



Appendix 7 Fig. 8
 Measured wall temps. from Steady Expts. 4 & 5 compared with predictions from
 two different CFD models
 [Qu, single channel model] Poro, porous medium model]

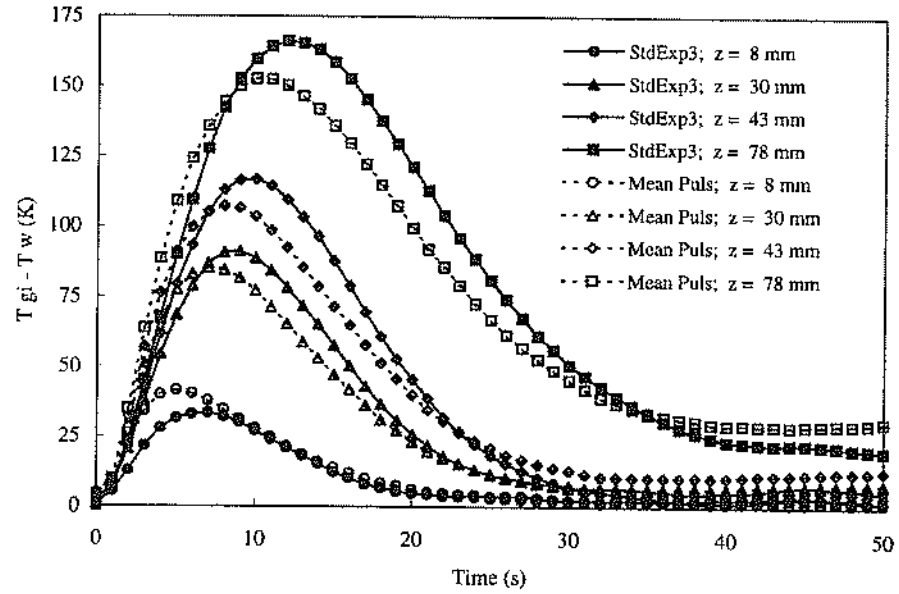


Appendix 7 Fig. 9
 Measured wall temps. from pulsing Expts. 1 & 2 compared with predictions from
 two different CFD models
 [Qu, single channel model] Poro, porous medium model]



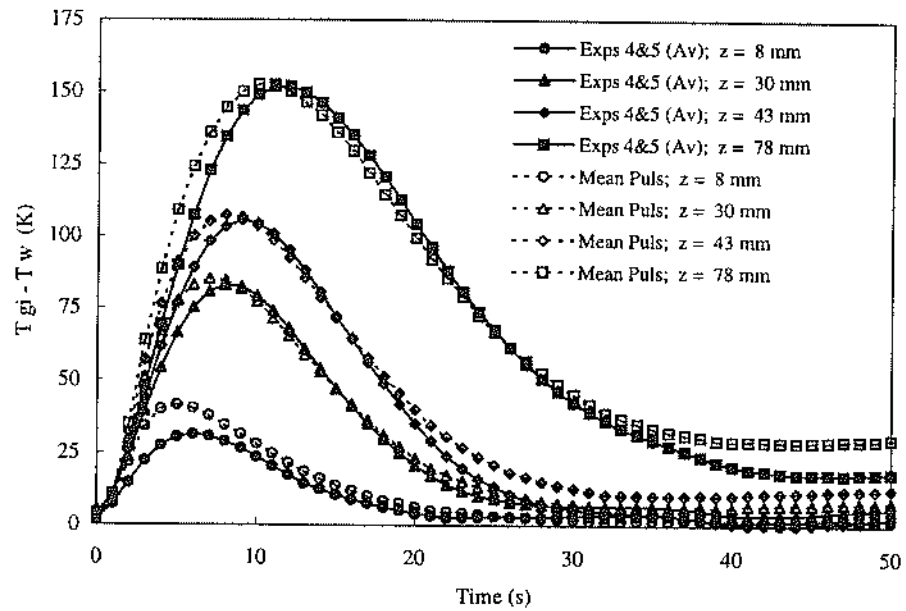
Appendix 7 Fig. 10

Comparison of steady flow (Expt. 3) with pulsed flow measurements (mean of Expts. 1 & 2)



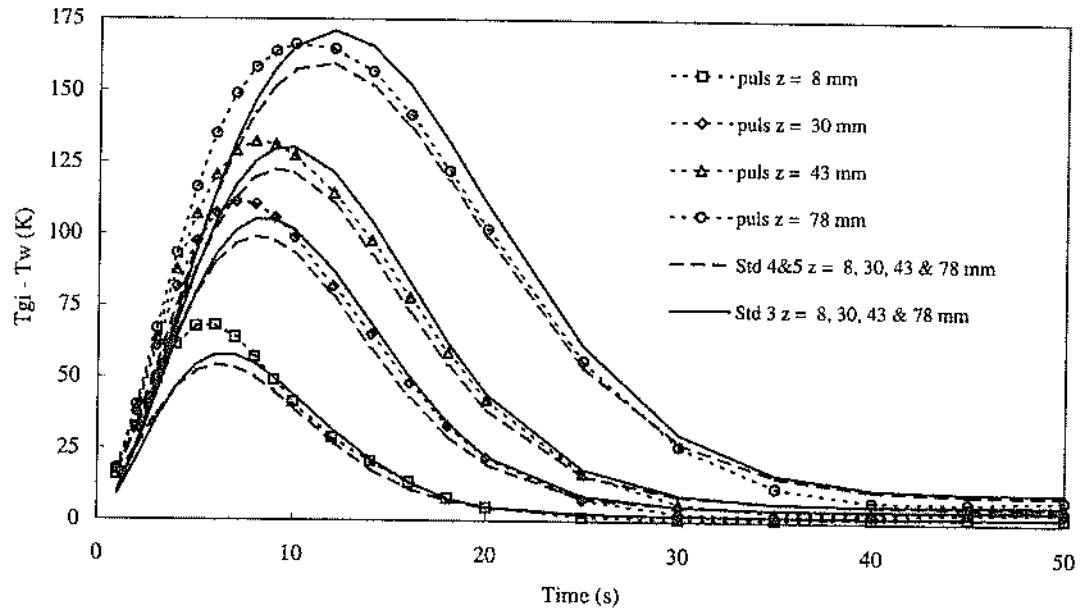
Appendix 7 Fig. 11

Comparison of steady flow measurements (mean of Expts. 4 & 5) with pulsed flow measurements (mean of Expts. 1 & 2)



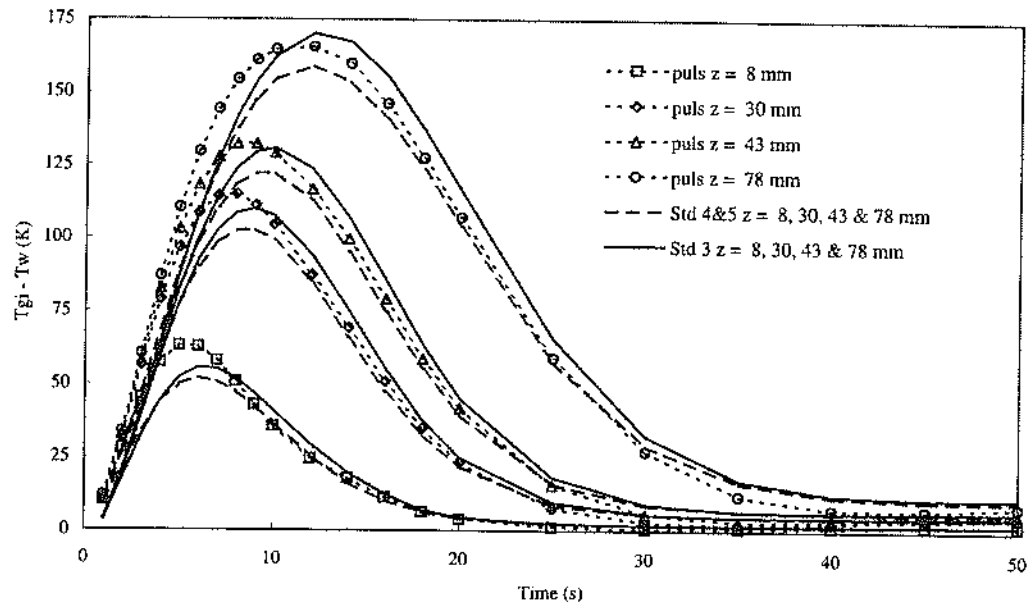
Appendix 7 Fig. 12

Predicted values of $T_{in} - T_{wall}$ (K) from the porous medium model for pulsing and steady cases

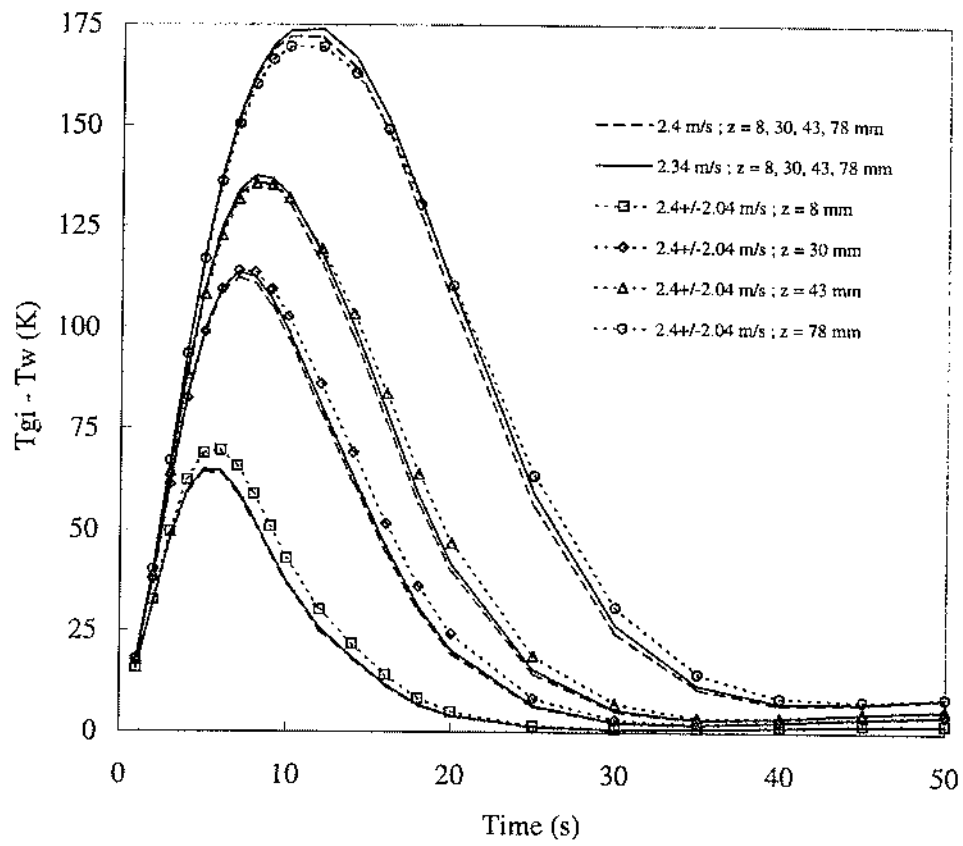


Appendix 7 Fig. 13

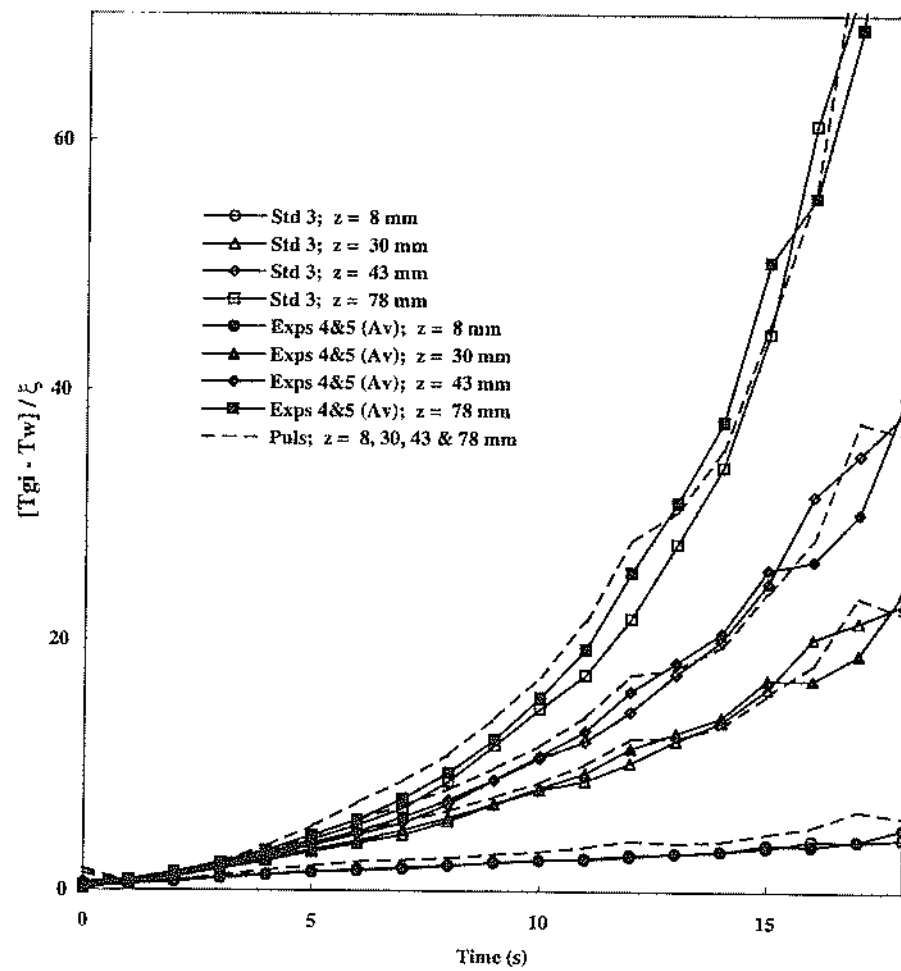
Predicted values of $T_{in} - T_{wall}$ (K) from quarter single channel model for pulsing and steady cases



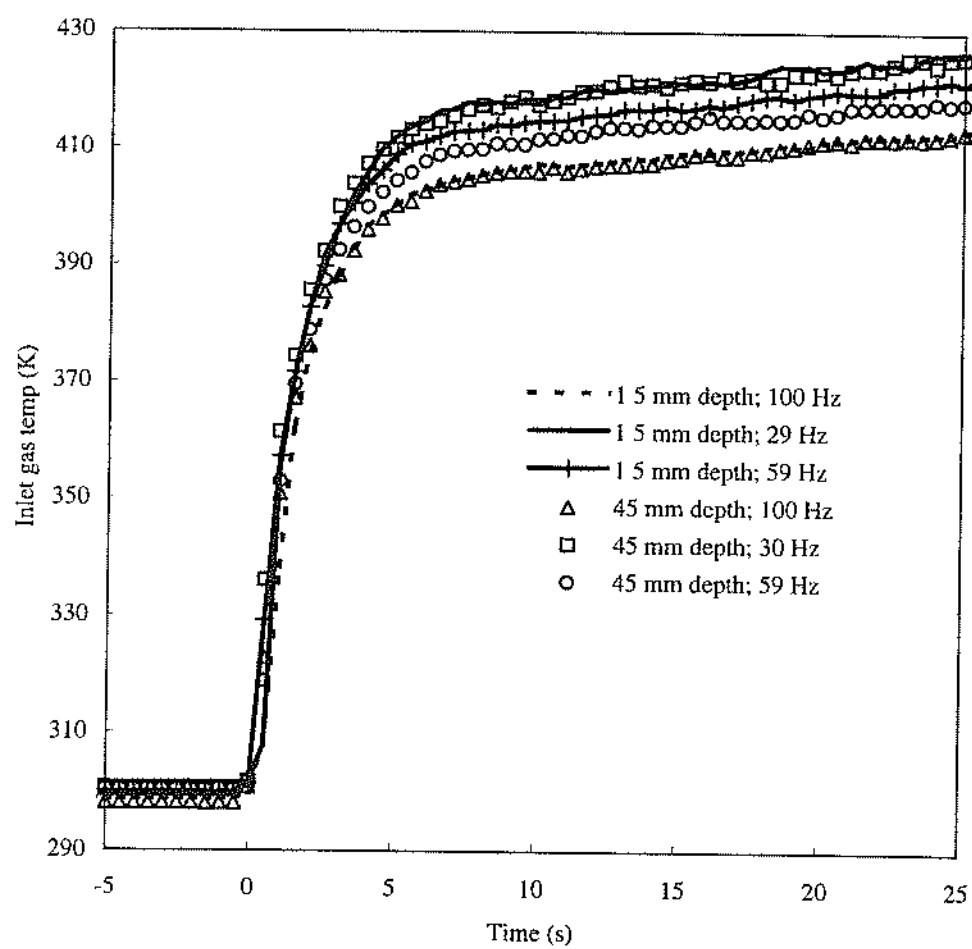
Results from porous medium model simulations using the inlet temperature ramp corresponding to the pulsing case; 2.34 and 2.4 m/s steady flow compared with 2.4 m/s pulsing flow



Plot of experimental data for $[T_{in} - T_{wall}] / \text{rate of rise of gas inlet temperature}$ for steady and pulsing cases

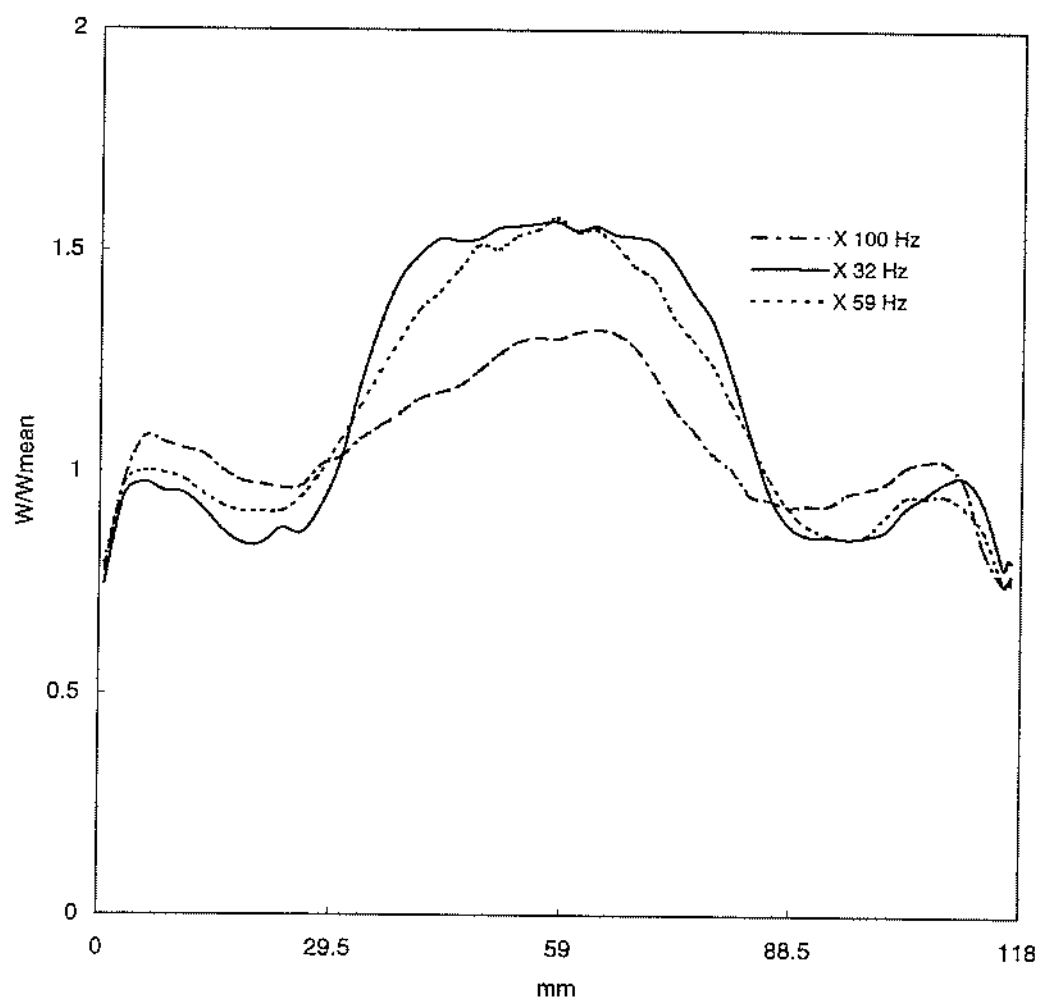


Inlet air temperature ramps for studies with conical diffuser



Appendix 7 Fig. 17

Velocity profiles at substrate exit, normalised to mean velocity



Appendix 7 Fig. 18

Ratio (equation 15) as a function of time

